Hindawi
Mathematical Problems in Engineering
Volume 2023, Article ID 6124793, 15 pages
https://doi.org/10.1155/2023/6124793

Research Article

Machining Characteristics Investigations of DSS-2205 Using RSM–ANN and Gray Relational Analysis

Endalkachew Mosisa Gutema and Mahesh Gopal

Department of Mechanical Engineering, College of Engineering and Technology, Wollega University, Post Box No: 395, Nekemte, Ethiopia

Correspondence should be addressed to Endalkachew Mosisa Gutema; endalkachewm@wollegauniversity.edu.et

Received 5 August 2022; Revised 8 November 2022; Accepted 13 November 2023; Published 5 December 2023

Academic Editor: Daniela Boso

DSS has low machinability characteristics due to its high strength, machining is complicated, and careful attention is required when selecting machining parameters. The main criteria discussed in this paper concern the turning optimization parameters and machining time reduction of DSS 2205 as the work material. The input parameters are cutting velocity, feeds, cutting depth, and tooltip nose radius of the cutting tool. The design of experiments methodology is employed to design the experiments using Design-Expert V12 software. The second-order mathematical model was developed, and analysis of variance was performed to analyze the performance characteristics to recognize the critical variables influencing the output parameter. An artificial neural network (ANN) backpropagation algorithm using MATLAB software was used to develop the mathematical model and optimize the output. The model was developed, and the results were optimized using MATLAB software's ANN back propagation method to find the best possible solutions. The generated models were significant based on the analysis of variance and the *R*-squared value, and these results indicate that the cutting velocity is the most critical factor. For a low machining time, the cutting velocity should be between 100 and 140 m/min, and the tooltip nose radius should be 2.8 mm. The optimal parameter settings are validated by performing a lower is better confirmation test using gray relational analysis (GRA). The GRA exposed the lower machining time at a cutting velocity of 140 m/min, rate of feed of 0.5 mm/rev, cutting depth of 0.5 mm, and tooltip nose radius of 2.4 mm. The predicted values were close to the experimental values, and the result indicates the optimal level of the highest GRA grade of the machining variable.

1. Introduction

Germany and Sweden invented the 22% Cr composition of duplex grade S32205 in the 1970s. It is essential to maintain nitrogen concentration; the heavily alloyed duplex grade was designed in the 1980s as the so-called super duplex grade. After the advancement, the scientists developed a lean alloy grade, DSS 832304. Alloying with nitrogen inspired the scientists to introduce many DSS grades. Despite its high yield strengths and high ductility properties, the producers and end-users have more significant restrictions during machining and welding [1]. DSS has the best mechanical properties and the highest resistance to chloride corrosion due to its progressive ductile–brittle transition and combined austenite and ferrite microstructure [2].

Palanisamy and Selvaraj [3] used cast DSS to assess the roughness of the workpiece and suggested that changing the grain orientation of the working materials had the most significant effect on the surface. Krolczyk et al. [4] examined the cutting performance of cutting tools MM 2025 and CTC 1135 during the machining of DSS 1.4462 material under dry and wet circumstances. The result revealed a minor difference in the effect of cooling on the material surface of the tools. The focus of the research is to forecast the roughness of the DSS material during the turning operation. The author derived the equations, and the results emphasize that the feed rate was the most critical factor affecting roughness [5]. Krolczyk et al. [6] derived a technique to estimate the life of the cutting tool during the turning of DSS material. The response surface methodology (RSM) technique creates a second-order model to predict equations for tool life and the results; cutting velocity was the crucial factor affecting the tool's life. The facing operation is performed under a constant cutting speed using austenitic, standard DSS, and super DSS material. Optimization was carried out using the Taguchi L16 orthogonal array technique. Koyee et al. [7] explained that the snarl and ribbon chips were created at lower feeds and higher cutting depths while milling super DSS and standard DSS forms. Fragments produced by milling austenitic stainless steel are machine-friendly, reducing ribbon, knotted, and flat helical chips.

Using the infinite focus measurement machine, Krolczyk and Legutko [8] investigated the surface texture and tool wear on DSS material. The author explained that when the feed rate increases, surface roughness also increases, and dry cutting enhances roughness and material ratio characteristics. The STD DSS, SDSS material, and carbide inserts coated with CNMG120408-QM 2025 were used as the cutting tool for experimentation. The author used a multiobjective bat algorithm (MOBA) to optimize the turning topographies. The MOBA regularly predicts a set of optimal solutions [9]. Analysis of variance (ANOVA) was used to investigate the performance characteristics of three DSS materials utilizing the mathematical model. Multiattribute decision-making has been used, including graph theory and matrix approach and analytical hierarchy process–technique for order preference by similarity to ideal solution, for optimization purposes [10]. Koyee et al. [11] developed prediction model experiments in dry and cooling lubricating conditions and compared them with cutting fluids and dried-out turning to lengthen tool life.

To determine the most effective machining method and cutting circumstances, Krolczyk et al. [12] employed DSS 1.4462 using the optimization techniques of ANOVA and Taguchi's orthogonal array L18. The influence of cutting speed, feed rate, depth of cut, and tool nose radii are studied using Taguchi's approach and ANOVA method to minimize surface waviness and material removal rate (MRR) [13]. The effects of surface and tool wear during the turning of DSS material in a traditional turning machine were investigated by Liew et al. [14]. Surface roughness decreased due to chilled air coolant instead of predictable coolant as the chilled air coolant's temperature fell, consequently affecting the surface roughness. Nomani et al. [15] explored the machined surface process and machinability of different components, specifically DSS alloys, SAF 2205 and SAF 2507, using scanning electron microscopy and optical microscopic examination. Pawan and Misra [16] considered DSS material for experimentation to predict roughness. To assess the surface waviness of the DSS material, Selvaraj [17] used the Taguchi approach. This study focuses on the impact of physical vapor deposition coatings on surface roughness and residual stresses at the cutting temperature during the DSS 2205 turning. The study investigated the residual stresses and surface unevenness impacted by coated and uncoated carbide tools. Sonawane and Sargade [18] suggested that the surface roughness of a machined surface can be improved by increasing the cutting speed. To measure surface roughness and machining time, experiments are conducted on duplex 2205 using a CNC lathe and carbide tip tool material under hard turning. A second-order mathematical model was developed using RSM, and performance characters were evaluated using the ANOVA method. The MOGA method was employed to achieve the most practical responses [19]. Kara et al. [20] experimented with AISI D2 hard turning under a cryogenic environment to assess the surface roughness and tool wear.

The reality of Duplex stainless steel is that it is resistant to chloride stress corrosion cracking. DSS material is twice more robust, low ductility than other austenitic grades. Duplex stainless steels are primarily utilized in specialized applications due to their limitations, which include poor formability and machinability and a more sophisticated metallurgical manufacturing process than ferritic, austenitic, and martensitic stainless steels. Therefore, careful consideration should be taken during the machining process. The literature indicates that the artificial neural network (ANN) heuristic method is suitable for enhancing the response optimization processes during the machining of Duplex grades. Even though numerous studies have been conducted, several types of research are available to predict surface roughness, tool wear, cutting force, and machinability analysis by using various optimization techniques during the turning of Duplex material. However, there is limited research available to optimize machining time using ANN on DSS material, and there is a significant gap in acknowledging and predicting machining time during the turning of DSS. Experimentation was conducted to overcome machining challenges and solve the critical concerns of industry specialists. The experiment was planned following the design of experiments (DoE) of central composite rotatable design (CCD). RSM and ANOVA were used to develop the mathematical models. The ANN, a heuristic optimization technique, was used.

2. Experimentation Details

The objective of this study was to determine the ideal machining conditions by estimating the optimal machining time during the turning of Duplex stainless steel (DSS-2205- ASTM A276) and by evaluating the impact of the cutting parameters. The cutting operation was carried out using a conventional Kirloskar Lathe using a coated carbide insert tool (Tungaloy—SNMG 120 408 MT AH925). The Duplex-2205 round bar of length 60 mm was used for experimentation. The parameter considered is cutting velocity (V_c), rate of feed (F_z), cutting Depth (D_c), and tooltip nose radius (R_{tip}). The experiments are designed per the central composite design, consisting of four-factor, five levels of the experiment using Design Expert Version 12 (stat case). The sample workpiece was machined to 20 mm, and a stopwatch was used to record the machining time. The Design for experimentation is shown in Table 1. The experimental results are tabulated in Table 2.

3. Identification of Design Matrix

The central composite experiment, i.e., CCD of RSM, is designed per the guidance given by Okouzi et al. [21]. Each component is allocated to five equally spaced values, typically coded as per the procedure of Box and Draper [22]. The experiment consists of four variables, five levels of CCD,

Table 1: Response table of process parameters.

Levels	Cutting velocity (V_c /m/min)	Rate of feed (F_z / mm/rev)	Cutting depth (D_c / mm)	Tooltip nose radius (R_{tip} / mm)
−2	80	0.2	2.5	0.8
−1	100	0.3	3.0	1.2
0	120	0.4	3.5	1.6
1	140	0.5	4.0	2.4
2	160	0.6	4.5	2.8

and experimental sets of actual states are shown in Table 1. The cutting condition ranges are selected from The IMOA Practical Guidelines Handbook [23]. Trial runs using the specified parameters generated to precise projected values given in Tables 1, the upper bound (+2) and the lower bound (2) levels of each of the four independent variables. The interpolation method was used to determine all intermediate variables levels 1, 0, and +1. A four-factor CCD with 30 sets of coded conditions of full replication, where 24 are non-center points and 6 are center points, was chosen as the design matrix to carry out the experiments using the DoE technique. Table 2 shows the 30 sets of coded trail experiments.

4. Regression Equations

Karthik et al. [24] conducted the regression analysis based on the DoE considering spindle speed, feed rate, and depth of cut under dry and wet conditions. According to the set of techniques provided by the authors. The 2nd-order quadratic mathematical regression models were developed for the parameters as follows:

$$\begin{aligned}T_m = {} & +5.58776 - 0.023294 \times V_c - 0.510281 \times F_z \\ & - 1.53034 \times D_c - 0.023342 \times R_{tip} - 0.010000 \times V_c \times F_z \\ & + 0.000500 \times V_c \times D_c - 0.002467 \times V_c \times R_{tip} + 0.525000 \\ & \times F_z \times D_c - 0.404018 \times F_z \times R_{tip} + 0.179911 \times D_c \times R_{tip} \\ & + 0.000125 \times V_c{}^2 + 0.393431 \times F_z{}^2 + 0.140737 \times D_c{}^2 \\ & - 0.043329 \times R_{tip}{}^2\end{aligned} \tag{1}$$

Regression equations are used to predict the machining time.

5. Results and Discussion

The Design-Expert V12 software is a statistical tool used to conduct experiments based on the DoE and examine the impacts of the response variable. The design matrix used to carry out the experiments is shown in Table 2. The ANOVA was performed to verify the adequacy of the model. The findings of an ANOVA used to predict T_m are shown in Table 3. Table 4 shows the percentage contribution of ANOVA.

The F value is 2.96, which is significant, and the P value is 2.26%, which may occur due to noise. The lack of fit (LF) F value is 0.2787, showing that the models' terms are not significant and have a noise of 95.54%.

6. Analysis of 3D Interaction Effect

The impact of process parameters cutting velocity (V_c), rate of feed (F_z), cutting depth (D_c), and Tooltip nose radius (R_{tip}) on machining time (T_m) is addressed below.

The interaction effect of cutting velocity and rate of feed on machining time is shown in Figure 1. The cutting velocity versus the rate of feed over machining time, as shown in Figure 1, has a significant influence on the machined surface and tends to increase machining time in hard turning. Figure 1 illustrates that when cutting velocity increases, machining time also increases; the machining time is minimum between 100 and 140 m/min. The rate of energy lost, plastic expansion, and friction increases as cutting velocity increases. When the feed rate increases, the machining time also increases proportionally, as illustrated in Figure 1; this is due to the larger cutting zone area between the tool and the workpiece, so a large amount of heat is developed at the tooltip, propagating the tool wear. The results are verified using the ANOVA table. The result concludes that the cutting velocity is the most influencing variable compared to other parameters.

The cutting depth plays a vital role throughout the machining, as shown in Figure 2. The cutting depth increases and the machining time increases; as a result, the quantity of workpiece materials is reduced.

Figure 3 shows the machining time relationship between cutting velocity and tooltip nose radius. The 3D plot in Figure 3 shows the machining time is high when the nose radius is at 2.8 mm and low at 0.8 mm. Figure 4 depicts the relationship between predicted and actual values. It helps to identify the observations by showing a graph of observed values vs. predicted values. The data points are evenly divided along the 45° line.

7. ANN Optimization

Hariche et al. [25] demonstrated that a mathematical model that attempts to simulate the structure and functions of biological neural networks is called an ANN. In recurrent ANN, information travels in one direction and the opposite direction in artificial outputs. An ANN has three layers: source, hiding, and destination. According to the author, the source and destination layers are called nodes, while the hiding layer links the origin and destination [26]. Rajesh et al. [27] developed a predictive model using the ANN technique to optimize the machining parameter during the turning of Inconel 625. To reduce the number of experiments and time-consuming trials, five learning techniques were utilized in

Table 2: Experimentation and observation.

Experimental run	Factor 1	Factor 2	Factor 3	Factor 4	Output responses	Predicted by optimization software	
	Cutting velocity (V_c)	Feed rate (F_z)	Cutting depth (D_c)	Nose radius (R_{tip})	Experimental machining time (T_{mExp})	Predicted machining time (T_{mRSM})	Predicted machining time (T_{mANN})
1	120	0.4	3.5	1.6	1.54	1.52	1.5101
2	100	0.5	3	1.2	1.46	1.49	1.4576
3	140	0.5	3	1.2	1.56	1.50	1.5155
4	100	0.3	4	2.4	1.61	1.59	1.5872
5	120	0.4	4.5	1.6	1.52	1.57	1.5179
6	100	0.3	3	2.4	1.48	1.50	1.4801
7	140	0.5	4	1.2	1.53	1.51	1.5101
8	140	0.3	4	2.4	1.61	1.59	1.5971
9	120	0.4	3.5	1.6	1.51	1.43	1.4201
10	120	0.4	3.5	1.6	1.47	1.42	1.4301
11	140	0.5	4	2.4	1.54	1.50	1.5224
12	120	0.4	3.5	1.6	1.36	1.42	1.4201
13	80	0.4	3.5	1.6	1.58	1.59	1.5841
14	120	0.4	3.5	1.6	1.37	1.42	1.3701
15	100	0.5	4	1.2	1.51	1.47	1.4908
16	120	0.4	3.5	1.6	1.28	1.42	1.3301
17	140	0.3	3	1.2	1.61	1.60	1.5811
18	120	0.6	3.5	1.6	1.35	1.39	1.3463
19	140	0.3	4	1.2	1.52	1.50	1.5106
20	100	0.3	3	1.2	1.53	1.51	1.5149
21	140	0.5	3	2.4	1.25	1.28	1.2551
22	100	0.5	4	2.4	1.57	1.58	1.5714
23	120	0.4	2.5	1.6	1.53	1.55	1.5092
24	100	0.5	3	2.4	1.44	1.38	1.3867
25	120	0.2	3.5	1.6	1.45	1.47	1.4171
26	100	0.3	4	1.2	1.41	1.39	1.3741
27	160	0.4	3.5	1.6	1.59	1.64	1.6082
28	120	0.4	3.5	2.8	1.32	1.37	1.3090
29	140	0.3	3	2.4	1.51	1.48	1.4959
30	120	0.4	3.5	0.8	1.34	1.38	1.3323

Table 3: Analysis of variance to predict—T_m.

Source	S.S.	df	M.S.	F	p	
Model of experiment	0.2183	14	0.0156	2.96	0.0226	Significant
Residual error	0.0789	15	0.0053	—	—	—
Lack of fit (LF)	0.0282	10	0.0028	0.2787	0.9594	Not significant
Pure error (PE)	0.0507	5	0.0101	—	—	—
Cor total	0.2972	29	—	—	—	—

Table 4: Percentage contribution of ANOVA.

Cutting parameters	Sum of squares	Degree of freedom	Mean square	F-ratio	% Of contribution
A—Cutting velocity	0.0192	1	0.0192	3.65	56.804
B—Rate of feed	0.0002	1	0.0002	0.0290	00.592
C—Cutting depth	0.0140	1	0.0140	2.65	41.420
D—Tool tip nose radius	0.0004	1	0.0004	0.0779	01.183
Total	0.0338	4	—	—	100

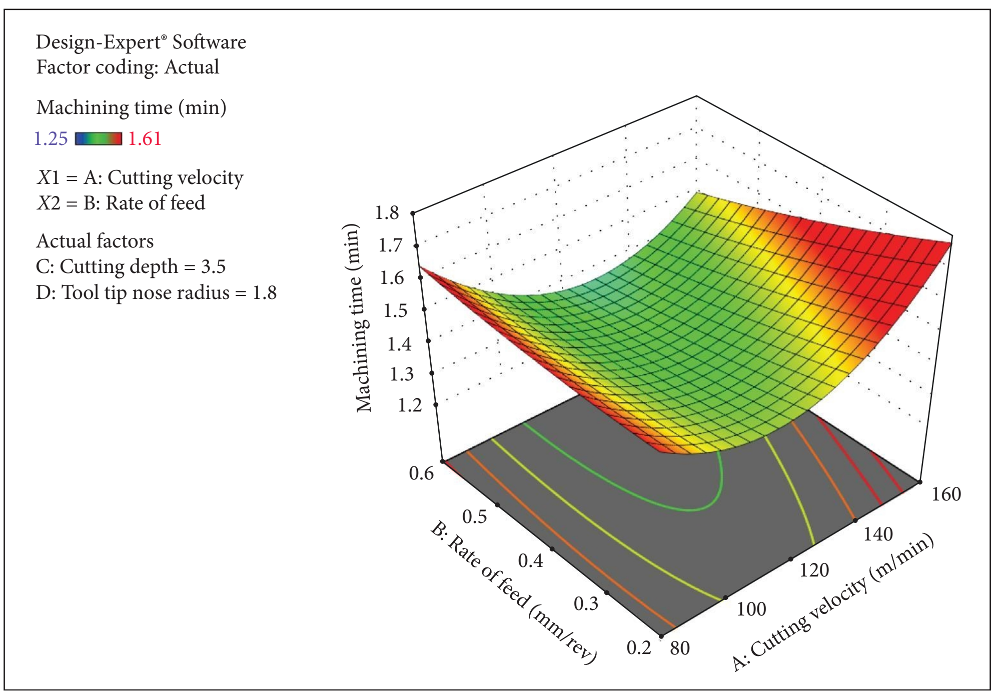

Figure 1: 3D plots (V_c versus F_z) over T_m.

ANN models to forecast the damage factor [28]. Eser et al. [29] used ANOVA and RSM to develop a prediction model to forecast surface roughness during the milling of AA6061 alloy. The ANN model was employed to identify the optimum machining conditions and evaluate the cutting parameters' impact. Manoj et al. [30] suggested that the ANN technique was the most effective method for the prediction of response parameters and also reduced the error percentage.

ANNs may solve complicated real-world issues by processing fundamental building blocks in nonlinear, distributed, parallel, and local ways. An ANN model is developed using the MATLAB NN tool.

The use of ANN to reduce machining time is described:

$$\text{To Minimize} : T_m\left(V_c, F_z, D_c, R_{tip}\right) \quad (2)$$

within limits,

(i) $90\,\text{m/min} \leq V_c \leq 120\,\text{m/min}$,
(ii) $0.18\,\text{mm/rev} \leq F_z \leq 0.36\,\text{mm/rev}$,
(iii) $0.20\,\text{mm} \leq D_c \leq 0.60\,\text{mm}$,
(iv) $0.40\,\text{mm} \leq R_{tip} \leq 0.80\,\text{mm}$.

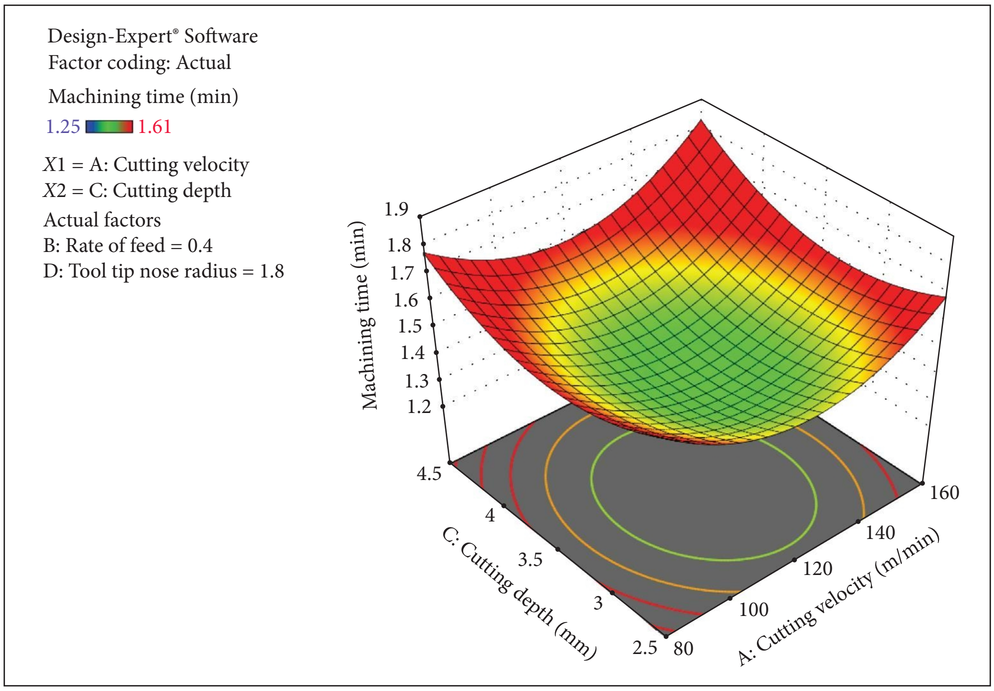

Figure 2: 3D plots (V_c versus D_c) over T_m.

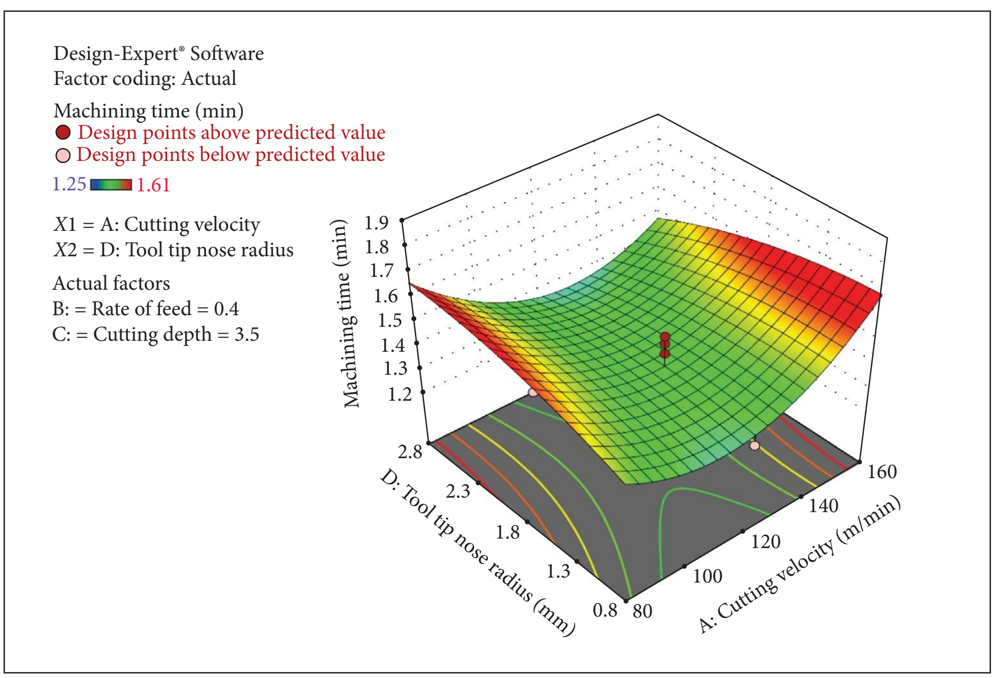

Figure 3: 3D plots (V_c versus R_{tip}) over T_m.

Subhash et al. [31] investigated the machinability and unstable process-induced chatter vibrations of dry-turning SDSS.

The input and output parameters will be trained using the ANN technique. The inputs, hidden, and output layers of the ANN levels are 1, the input layer unit is 4, the hidden layer and output layer unit is 5, and Epochs are 1,000. The back propagation neural network algorithm (gradient descent learning rule) was used for processing ANN. The sigmoid activation function was used to train the neural network model.

Figure 5 shows the machining time ANN structure, and Figure 6 depicts the input, hidden, and output layers used in the ANN model. The machining time was estimated using the NN trainer, which drives through 1,000 repetitions, as shown in Figure 7. Figures 8 and 9 show the regression plot and ANN validation performance; these show the gradient, validation check, and learning rate. Figure 10 shows the

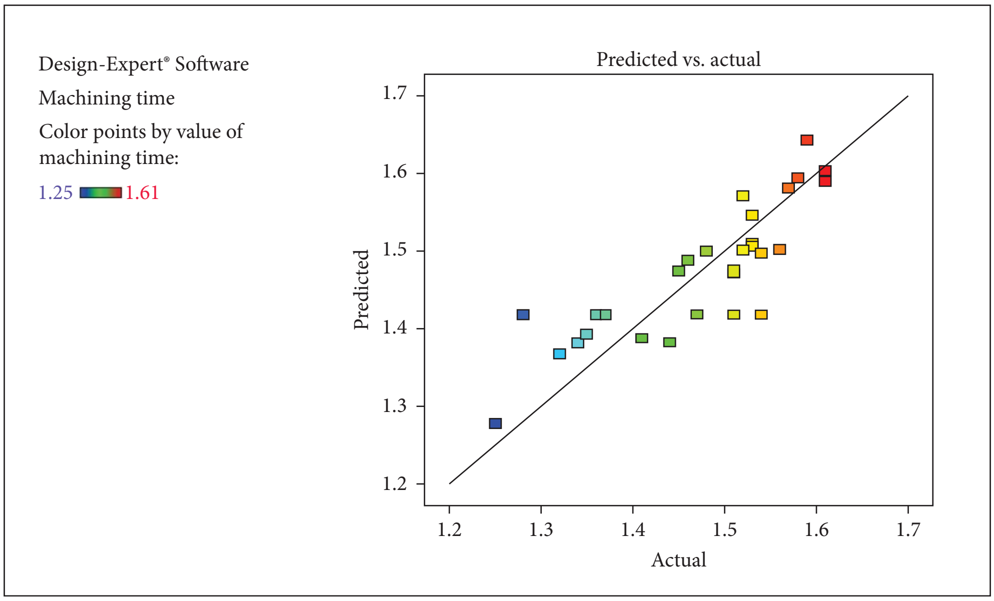

Figure 4: Predicted versus actual result.

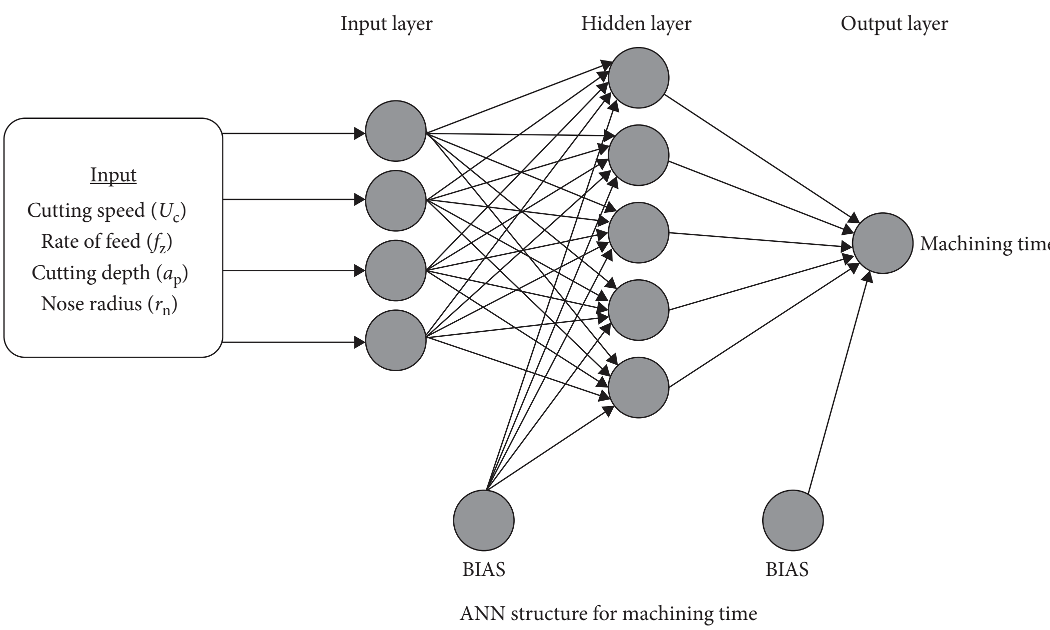

Figure 5: ANN structure for machining time.

results of ANN validation performance; these show that the training, validation, and testing using ANN are very close to the predicted values.

The output of experimental and trained ANN data is shown in Figure 11. This graph shows the experimental results obtained by using ANN are very close, and evaluations are accurate to their values. The output of experimental, RSM, and trained ANN data are shown in Figure 12. This graph shows that the experimental, RSM result obtained from Design Expert software and ANN result are adjacent to their output values. Figure 13 shows the error percentage between RSM and ANN over the experimental value. The ANN predicted values show the lowest deviation than RSM values. The ANN was successfully trained for better prediction than RSM.

8. Validation of the Model Using ANN Transfer Functions

Various types of standardized statistical performance evaluation criteria are used to assess and validate the models applied in ANNs. Three different kinds of transfer functions have been used for neurons in hidden layers: hyperbolic tangent sigmoid (TANSIG), log sigmoid (LOGSIG), and PURELIN are compared and investigated for improving the performance of the proposed neural networks [32–34].

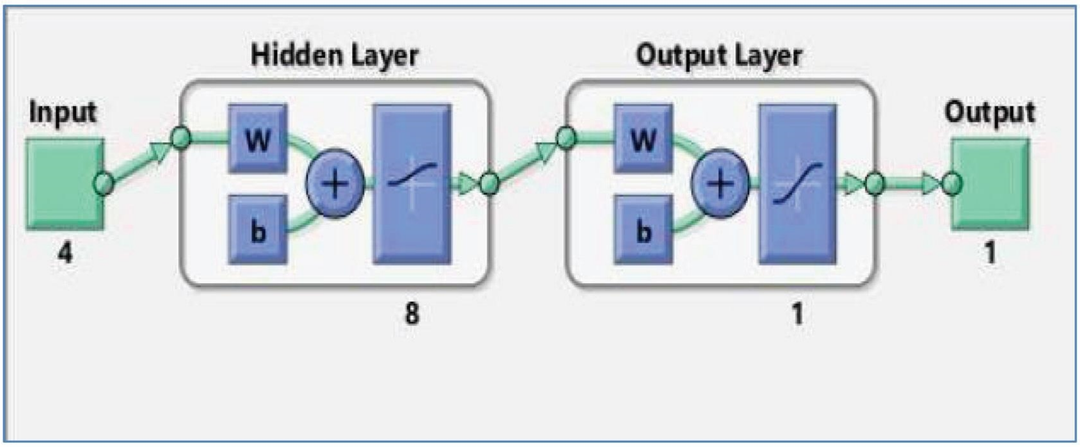

Figure 6: The input, hidden, and output layer.

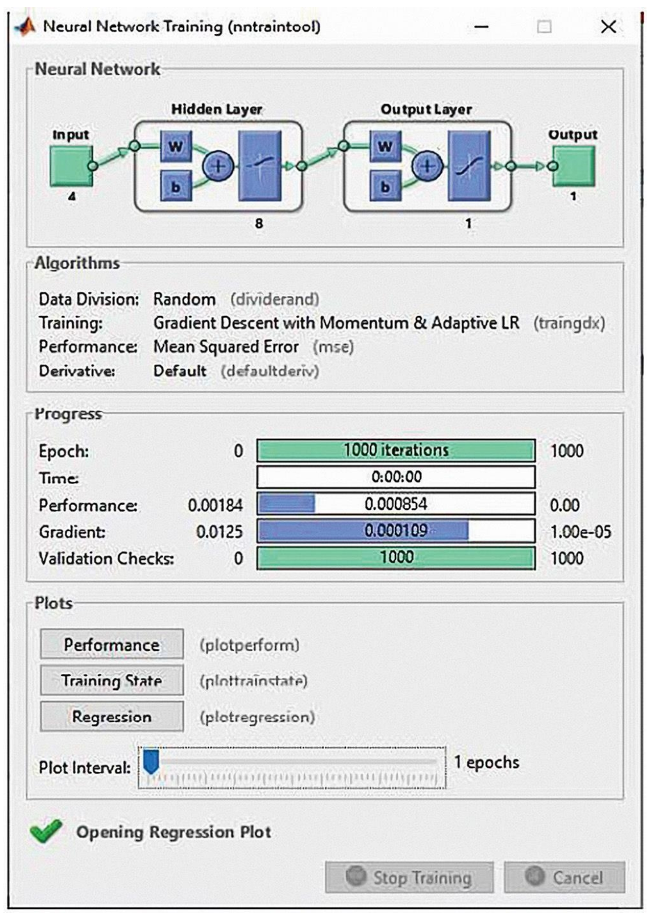

Figure 7: Neural network training.

The ANN is trained by transfer functions using scaled gradient Descent with Momentum & Adaptive L.R. method. TANSIG and purely transfer function models are trained in the ANN network to compare whether the model is efficient and provides less predicted value. The 15 datasets are selected for testing. The results are compared; the LOGSIG is the most suitable transfer function that reflects the minimum prediction result. The predicted value of the three transfer functions is shown in Table 5. The validation result is shown in Table 6.

9. Validation Using Gray Relational Analysis (GRA)

GRA is an efficient approach for maximizing the complex interrelationships between multiple performance variables. Prasad

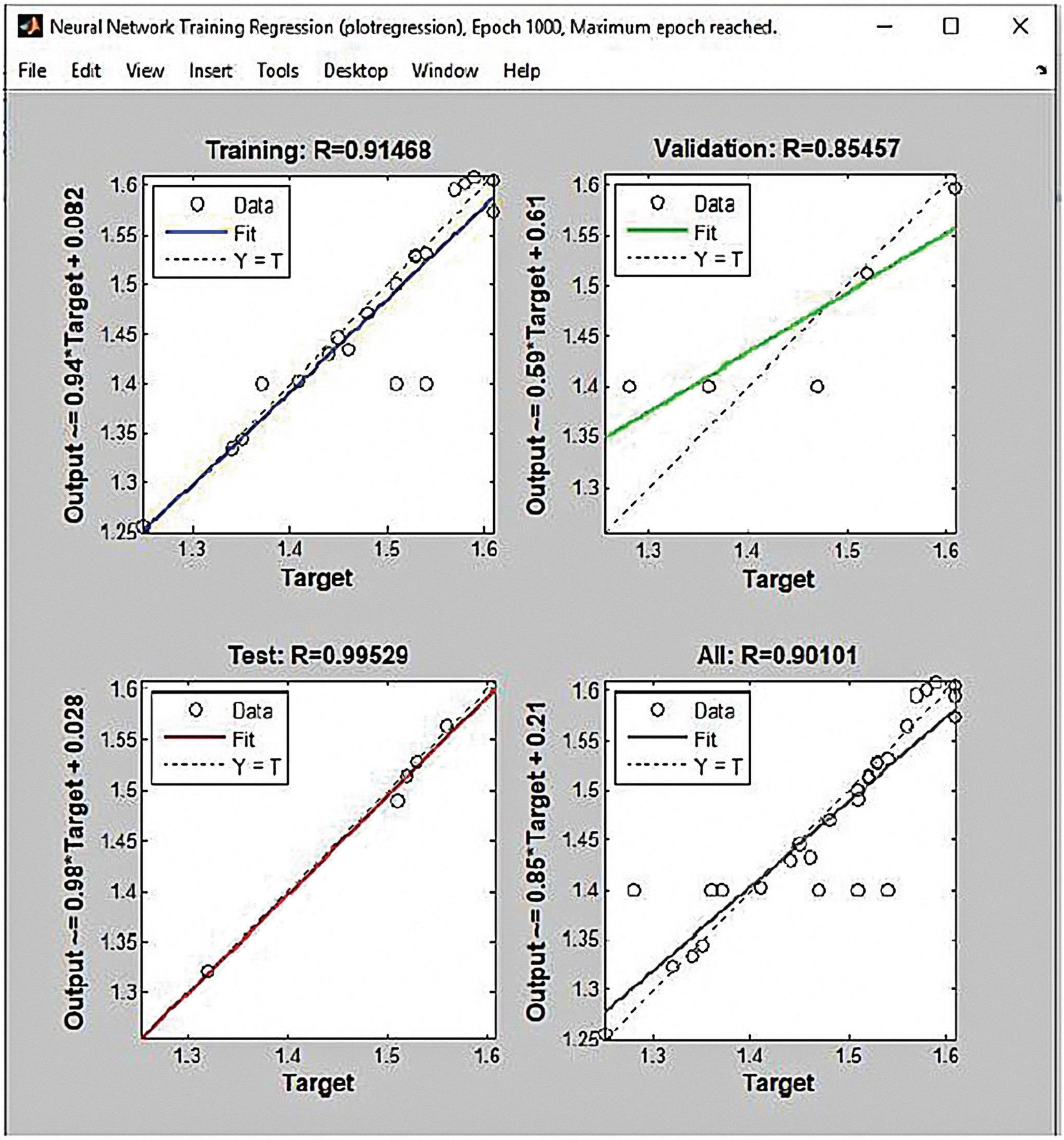

Figure 8: Plot regression.

et al. [35] proposed the GRA technique to optimize the pulsed current MPAW process, considering quality factors. Srivastava et al. [36] utilized a combination of RSM and GRA approaches to improve the process parameters of the FDM. GRA was used to handle the multiresponse optimization problem by altering the weights for distinct replies based on the quality or productivity needs of the process [37]. Kirti and Raju [38] studied how to use GRA to optimize the WEDM process parameters of Inconel 600 with other performance attributes. Deng [39] proposed GRA based on the gray system theory to solve the intricate interrelationships among several responses.

The objective is to reduce machining time. The procedures are mentioned as follows:

(1) The experimental values were first normalized from 0 to 1.

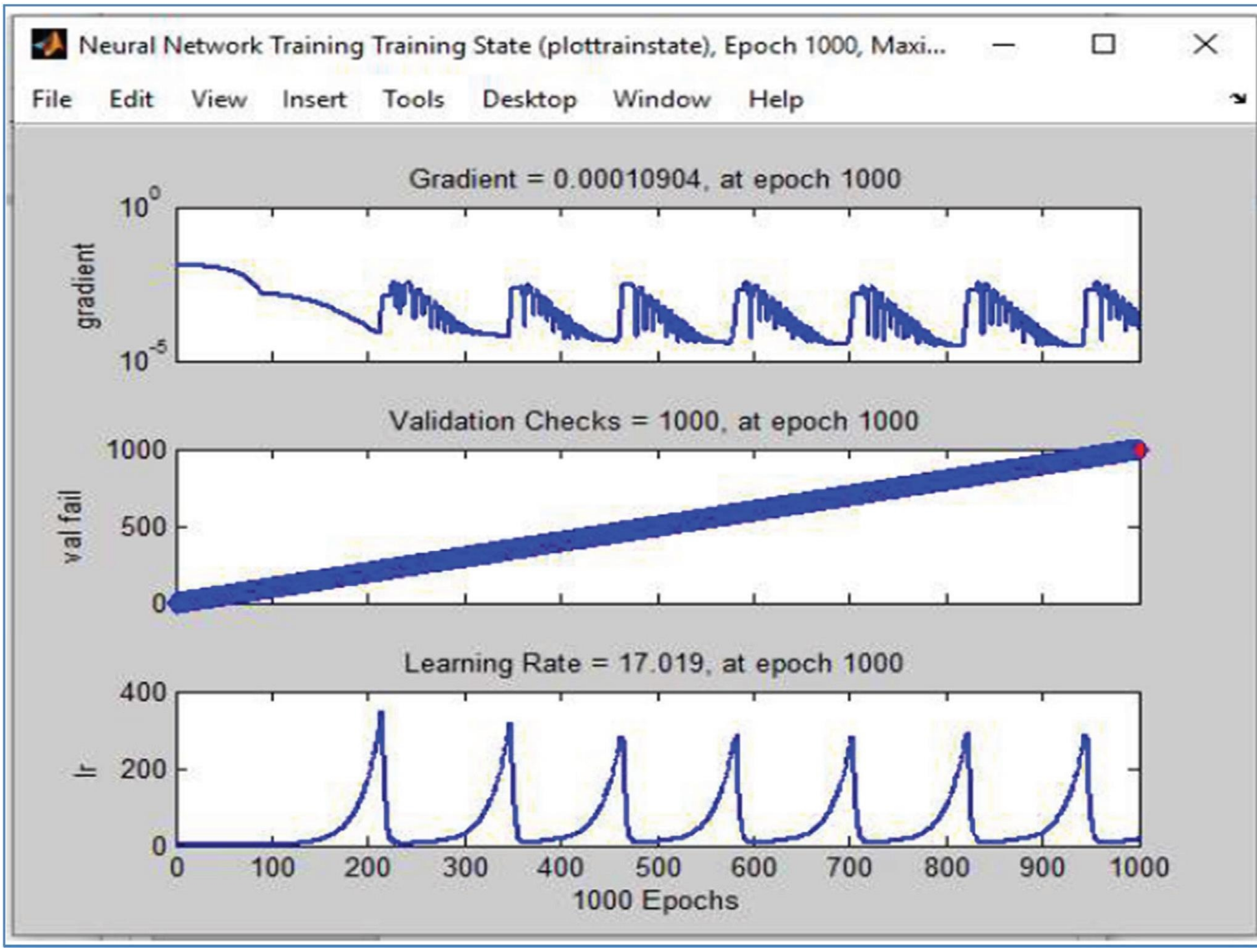

Figure 9: Plot train state (1,000 epoch).

(A) Smaller-the-better criteria

$$y_i(m) = \frac{\max(x_i(m)) - x_i(m)}{\max(x_i(m)) - \min(x_i(m))}, \tag{3}$$

(B) Higher-the-better criteria

$$y_i(m) = \frac{x_i(m) - \max(x_i(m))}{\max(x_i(m)) - \min(x_i(m))}, \tag{4}$$

where $y_i\ (m)$ is the value after gray relational generation; min $x_i\ (m)$ is the smallest value of $x_i\ (m)$ for the mth response; max $x_i\ (m)$ is the largest value of $x_i\ (k)$ for the mth response.

(2) The gray relational coefficient (γ) was computed using normalized experimental findings in the next phase.

$$\gamma_i(m) = \frac{\Delta_{\min} - \varepsilon\Delta_{\max}}{\Delta O_i(m) + \varepsilon\Delta_{\max}}, \tag{5}$$

where γ_i is the distinguishing coefficient: if γ is smaller, then the distinguishing ability is larger. In common, $\gamma = 0.5$ is used; $\Delta_{\min}$ represents the smallest value of $\Delta O_i\ (m)$; $\Delta_{\max}$ represents the largest value of $\Delta O_i\ (m)$, ε represents the distinguishing coefficient.

(3) The overall gray relational grade (GRG) was calculated by averaging the gray relational coefficients for each chosen response.

$$X_i = \frac{1}{n}\sum_{m=1}^{n} w_k\gamma_i(m), \tag{6}$$

where X_i represents the overall GRG; w_k represents the normalized weightage of factor m.

The relevance of factors with uneven weightage is borne by diverse aspects of a simple engineering system.

The primary purpose of this research is to minimize machining time. As a result, GRA optimization, the “lower is better” approach, was applied. To begin, trial data were standardized using Equation (3) to achieve gray relational generation, as tabulated in Table 7. The GRA coefficient (γ) was computed from normalized experimental results using Equation (5). The overall GRA grade (X_i) was calculated by averaging the GRA coefficients for each selected response. For all of the processing, variables are weighted;

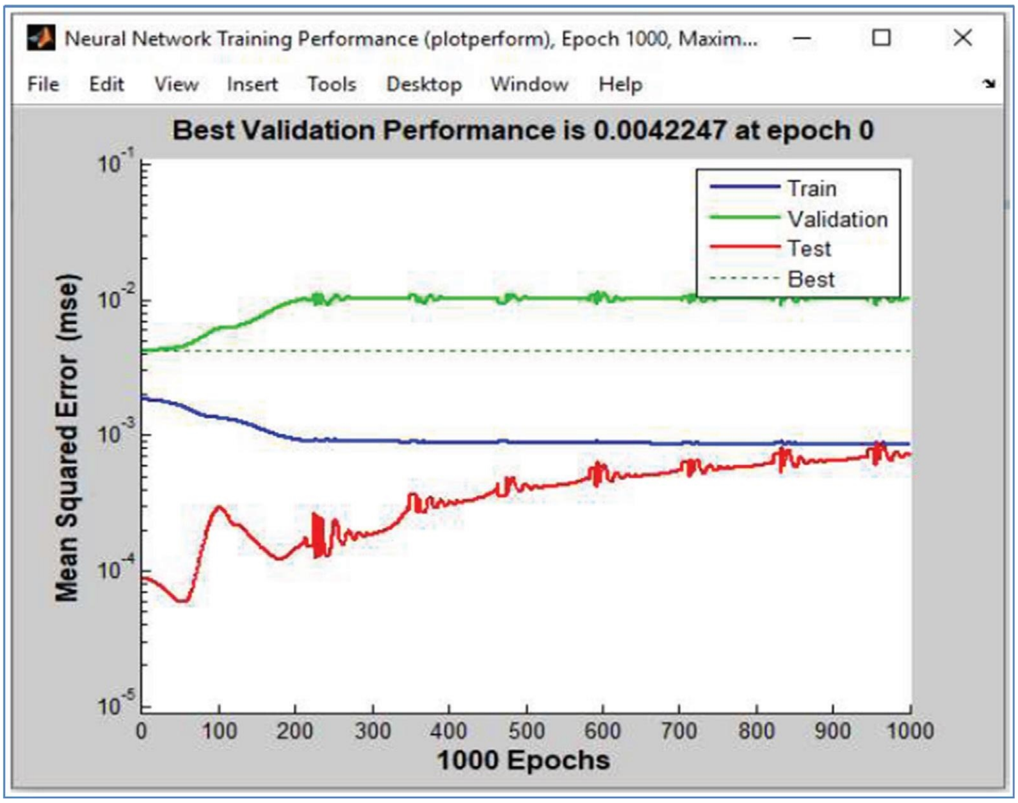

Figure 10: ANN validation performance.

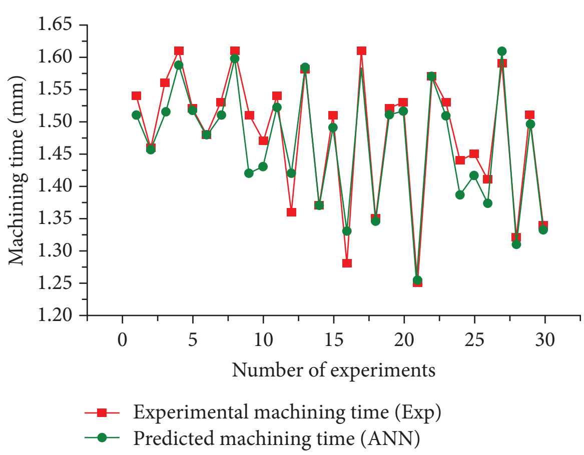

Figure 11: Output comparison—trail (experimental) and ANN data.

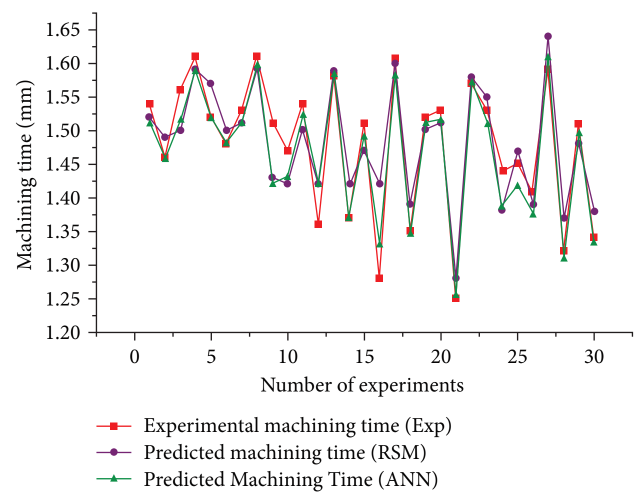

Figure 12: Output comparison—RSM, ANN, trail (experiment) values.

equally, X_i equals 0.5. If all of the processing variables are weighted equally, X_i equals 0.5. Table 5 shows the overall gray relational rank. As a result, the level with the highest GRA grade value is the optimal level for the machining variables.

10. Conclusion

The turning operation was performed using DSS 2025 workpiece material and input factors: cutting velocity, rate of feed, cutting depth, and tooltip nose radius. The 2nd-order statistical model is developed to forecast machining time utilizing CCD and DoE of RSM. This method examines the interaction impact of the process parameter. A heuristic ANN is used to optimize and analyze the ANN model, which yields more accurate forecast data.

In terms of prediction, the findings demonstrate that the ANN outperforms the RSM.

The cutting velocity has the most significant influence compared to the other parameters, and the machining time is low when the cutting velocity of 100–140 m/min.

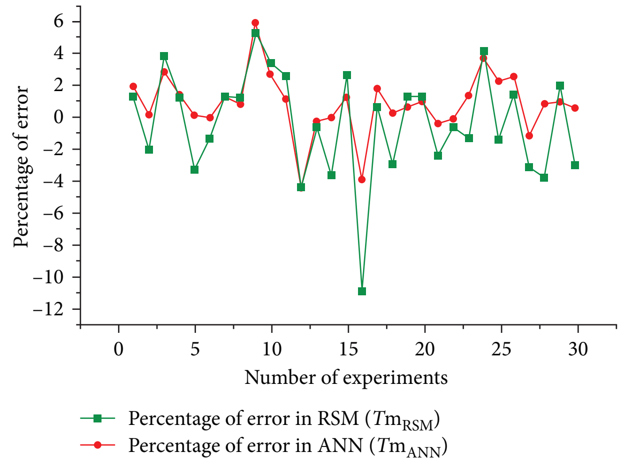

Figure 13: Comparison of RSM, ANN over % of trail (experiment) error.

Table 5: Prediction value of LOGSIG, PURELIN, and TRANSIG transfer functions.

Experimental run	Factor 1	Factor 2	Factor 3	Factor 4	Machining time (T_m) predicted by MATLAB software		
	Cutting velocity (V_c)	Feed rate (F_z)	Cutting depth (D_c)	Nose radius (R_{tip})	ANN_{LOGSIG}	$ANN_{PURELIN}$	ANN_{TANSIG}
16	120	0.4	3.5	1.6	1.3301	1.4210	1.4532
17	140	0.3	3	1.2	1.5811	1.5174	1.5826
18	120	0.6	3.5	1.6	1.3463	1.4101	1.4354
19	140	0.3	4	1.2	1.5106	1.5502	1.5845
20	100	0.3	3	1.2	1.5149	1.5375	1.5867
21	140	0.5	3	2.4	1.2551	1.2623	1.2731
22	100	0.5	4	2.4	1.5714	1.5802	1.5873
23	120	0.4	2.5	1.6	1.5092	1.5184	1.5247
24	100	0.5	3	2.4	1.3867	1.4603	1.4684
25	120	0.2	3.5	1.6	1.4171	1.4354	1.4432
26	100	0.3	4	1.2	1.3741	1.3747	1.3864
27	160	0.4	3.5	1.6	1.6082	1.6186	1.6201
28	120	0.4	3.5	2.8	1.3090	1.3124	1.3205
29	140	0.3	3	2.4	1.4959	1.5021	1.5122
30	120	0.4	3.5	0.8	1.3323	1.3487	1.3492
Average					1.4361	1.4566	1.4752

Table 6: Validation of ANN data transfer functions.

Sl. no	Transfer functions	The Max. predicted value of machining time	The Min. predicted value of machining time
1	LOGSIG function	1.6082	1.2551
2	PURELIN function	1.6186	1.2623
3	TANSIG function	1.6201	1.2731

To produce the optimum results, the nose radius of the cutting tool should be 2.8 mm. In the ANN optimization, the observed values and the ANN projected values correlate closely.

The results are further evaluated using GRA and exposed that the ideal machining settings are $V_c = 140$ m/min, $F_z = 0.5$ mm/rev, $D_c = 0.5$ mm, and $R_{tip} = 2.4$ mm.

The ANN and GRA results are the same; it is confirmed that ANN performs well. Confirmation tests were done using the GRA method and were validated for the performance measures. The anticipated data from the ANN has a margin of error of less. Consequently, the model is acceptable, and the optimum cutting parameters ensured significant

Table 7: Gray relational generations—analysis of turning data.

Sl. no	Normalization—smaller the better	Deviation sequence	Gray relational coefficients (GRC)	Rank
1	0.2162	0.7838	0.3895	22
2	0.4324	0.5676	0.4684	11
3	0.1622	0.8378	0.3737	24
4	0.0000	1.0000	0.3333	30
5	0.2703	0.7297	0.4066	17
6	0.3784	0.6216	0.4458	13
7	0.2432	0.7568	0.3978	19
8	0.0270	0.9730	0.3394	28
9	0.2973	0.7027	0.4157	14
10	0.4054	0.5946	0.4568	12
11	0.2162	0.7838	0.3895	22
12	0.7027	0.2973	0.6271	6
13	0.1081	0.8919	0.3592	26
14	0.6757	0.3243	0.6066	7
15	0.2973	0.7027	0.4157	14
16	0.9189	0.0811	0.8605	2
17	0.0270	0.9730	0.3394	28
18	0.7297	0.2703	0.6491	5
19	0.2703	0.7297	0.4066	17
20	0.2432	0.7568	0.3978	19
21	1.0000	0.0000	1.0000	1
22	0.1351	0.8649	0.3663	25
23	0.2432	0.7568	0.3978	19
24	0.4865	0.5135	0.4933	9
25	0.4595	0.5405	0.4805	10
26	0.5676	0.4324	0.5362	8
27	0.0811	0.9189	0.3524	27
28	0.8108	0.1892	0.7255	3
29	0.2973	0.7027	0.4157	14
30	0.7568	0.2432	0.6727	4

improvement in the machining time. The result of the experiment assists the industrialists in improving the performance measure by reducing the machining time, which saves the operator energy/cost and improves productivity.

11. Future Studies

Studies and experiments in the fields of machinability, impact toughness, MRR, etc., will be carried out in order to optimize the DSS 2025 machining process. To ascertain the effects of cutting fluids, MQL, and cryogenic machining, further research must be done. Modifying the nomenclature of the tools to guarantee precise machining. Future use of sustainable machining technology is possible to reduce environmental pollution.

Data Availability

The data used to support the findings of this study are included within the article.

Disclosure

This study was performed as a part of the employment of Wollega University, Nekemte, Ethiopia.

Conflicts of Interest

The authors declare that there are no conflicts of interest regarding the publication of this article.

Authors' Contributions

Methodology was done by Endalkachew Mosisa Gutema and Mahesh Gopal; Experiments and data analysis were done by Endalkachew Mosisa Gutema and Mahesh Gopal; Software-related task was done by Mahesh Gopal; Writing—Original draft preparation was done by Mahesh Gopal; Writing—Review and Editing was done by Endalkachew Mosisa Gutema. All authors have read and agreed to the published version of the manuscript.

References

[1] R. N. Gunn, *Duplex Stainless Steels: Microstructure, Properties, and Applications*, Abington Publishing, Cambridge, England, 1997.

[2] R. M. Davison and J. D. Redmond, "A guide to using duplex stainless steels," *Materials & Design*, vol. 12, no. 4, pp. 187–192, 1991.

[3] D. P. Selvaraj and P. Chandramohan, "Influence of cutting speed, feed rate and bulk texture on the surface finish of nitrogen alloyed duplex stainless steels during dry turning," *Engineering*, vol. 2, pp. 453–460, 2010.

[4] G. Krolczyk, S. Legutko, and A. Stoić, "Influence of cutting parameters and conditions onto surface hardness of duplex stainless steel after turning process," *Tehnički vjesnik*, vol. 20, no. 6, pp. 1077–1080, 2013.

[5] G. Krolczyk, S. Legutko, and M. Gajek, "Predicting the surface roughness in the dry machining of duplex stainless steel (DSS)," *Metalurgija*, vol. 52, no. 2, pp. 259–262, 2013.

[6] G. Królczyk, M. Gajek, and S. Legutko, "Predicting the tool life in the dry machining of duplex stainless steel," *Eksploatacja i Niezawodność–Maintenance and Reliability*, vol. 15, no. 1, pp. 62–65, 2013.

[7] R. D. Koyee, R. Eisseler, and S. Schmauder, "Application of Taguchi coupled fuzzy multi-attribute decision making (FMADM) for optimizing surface quality in turning austenitic and duplex stainless steels," *Measurement*, vol. 58, pp. 375–386, 2014.

[8] G. M. Krolczyk and S. Legutko, "Experimental analysis by measurement of surface roughness variations in turning process of duplex stainless steel," *Metrology and Measurement Systems*, vol. 21, no. 4, pp. 759–770, 2014.

[9] R. D. Koyee, U. Heisel, S. Schmauder, and R. Eisseler, "Experimental investigation and multi-objective optimization of turning duplex stainless steels," *International Journal of Manufacturing Engineering*, vol. 2014, Article ID 921081, 13 pages, 2014.

[10] R. D. Ali, *Modeling and optimization of turning duplex stainless steels*, Ph.D. ThesisInstitut für Werkzeugmaschinen der Universität Stuttgart, 2015.

[11] R. D. Koyee, S. Schmauder, U. Heisel, and R. Eisseler, "Numerical modeling and optimization of machining duplex stainless steels," *Production & Manufacturing Research*, vol. 3, no. 1, pp. 36–83, 2015.

[12] G. M. Krolczyk, R. W. Maruda, P. Nieslony, and M. Wieczorowski, "Surface morphology analysis of duplex stainless steel (DSS) in clean production using the power spectral density," *Measurement*, vol. 94, pp. 464–470, 2016.

[13] S. Dinesh, A. G. Antony, S. Karuppusamy, B. S. Kumar, and V. Vijayan, "Experimental investigation and optimization of machining parameters in CNC turning operation of duplex stainless steel," *Asian Journal of Research in Social Sciences and Humanities*, vol. 6, no. 10, pp. 179–195, 2016.

[14] P. J. Liew, U. S. Hashim, and M. N. Abd Rahman, "Effect of chilled air coolant on surface roughness and tool wear when machining 2205 duplex stainless steel," *Journal of Advanced Manufacturing Technology (JAMT)*, vol. 11, no. 1, pp. 61–68, 2017.

[15] J. Nomani, A. Pramanik, T. Hilditch, and G. Littlefair, "Chip formation mechanism and machinability of wrought duplex stainless steel alloys," *The International Journal of Advanced Manufacturing Technology*, vol. 80, pp. 1127–1135, 2015.

[16] K. Pawan and J. P. Misra, "A surface roughness predictive model for DSS longitudinal turning operation," in *DAAAM International Scientific Book*, B. Katalinic, Ed., pp. 285–296, DAAAM International, Vienna, Austria, 2018.

[17] D. P. Selvaraj, "Optimization of surface roughness of duplex stainless steel in dry turning operation using Taguchi technique," *Materials Physics and Mechanics*, vol. 40, pp. 63–70, 2018.

[18] G. D. Sonawane and V. G. Sargade, "Studies on the characterization and machinability of duplex stainless steel 2205 during dry turning," *International Journal of Mechanical and Industrial Engineering*, vol. 13, no. 5, pp. 349–353, 2019.

[19] M. Gopal, "Experimental investigation of duplex stainless steel using RSM and multi-objective genetic algorithm (MOGA)," in *Materials, Design, and Manufacturing for Sustainable Environment*, S. Mohan, S. Shankar, and G. Rajeshkumar, Eds., Lecture Notes in Mechanical Engineering, pp. 813–834, Springer, Singapore, 2021.

[20] F. Kara, M. Karabatak, M. Ayyıldız, and E. Nas, "Effect of machinability, microstructure and hardness of deep cryogenic treatment in hard turning of AISI D2 steel with ceramic cutting," *Journal of Materials Research and Technology*, vol. 9, no. 1, pp. 969–983, 2020.

[21] A. S. Okouzi, A. O. A. Ibhadode, and A. I. Obanor, "Response surface methodology (RSM) optimization of the batch process in a rectangular passive greenhouse dryer," *International Journal of Engineering Research in Africa*, vol. 56, pp. 145–161, 2021.

[22] G. E. P. Box and N. R. Draper, *Empirical Model-Building and Response Surfaces*, Wiley Series in Probability and Statistics, John Wiley, New York, 1987.

[23] International Molybdenum Associations (IMOA), *Practical Guidelines for the Fabrication of Duplex Stainless Steel*, International Molybdenum Associations (IMOA), London, UK, 2nd Edn edition, 2009.

[24] R. M. C. Karthik, R. L. Malghan, F. Kara, A. Shettigar, S. S. Rao, and M. A. Herbert, "Influence of support vector regression (SVR) on cryogenic face milling," *Advances in Materials Science and Engineering*, vol. 2021, Article ID 9984369, 18 pages, 2021.

[25] L. Hariche, B. Benahmed, and A. Moustafa, "Response spectrum with uncertain damping using artificial neural networks," *International Journal of Engineering Research in Africa*, vol. 56, pp. 136–144, 2021.

[26] M. Gopal, "The effect of machining parameters and optimization of temperature rise in turning operation of aluminium-6061 using RSM and artificial neural network," *Periodica Polytechnica Mechanical Engineering*, vol. 65, no. 2, pp. 141–150, 2021.

[27] A. S. Rajesh, M. S. Prabhuswamy, and I. K. Raghavan, "Modelling and analysis of surface roughness using the cascade forward neural network (CFNN) in turning of inconel," *Advances in Materials Science and Engineering*, vol. 2022, Article ID 7520962, 9 pages, 2022.

[28] Ö. Erkan, B. Işık, A. Çiçek, and F. Kara, "Prediction of damage factor in end milling of glass fibre reinforced plastic composites using artificial neural network," *Applied Composite Materials*, vol. 20, pp. 517–536, 2013.

[29] A. Eser, E. A. Ayyıldız, M. Ayyıldız, and F. Kara, "Artificial intelligence-based surface roughness estimation modelling for milling of AA6061 alloy," *Advances in Materials Science and Engineering*, vol. 2021, Article ID 5576600, 10 pages, 2021.

[30] I. V. Manoj, H. Soni, S. Narendranath, P. M. Mashinini, and F. Kara, "Examination of machining parameters and prediction

of cutting velocity and surface roughness using RSM and ANN using WEDM of Altemp HX," *Advances in Materials Science and Engineering*, vol. 2022, Article ID 5192981, 9 pages, 2022.

[31] N. Subhash, T. Jagadeesha, and M. Law, "Investigations on machinability and machining stability of turning super duplex stainless steel," *International Journal of Machining and Machinability of Materials*, vol. 22, no. 5, pp. 386–405, 2020.

[32] R. Sarkar, S. Julai, S. Hossain, W. T. Chong, and M. Rahman, "A comparative study of activation functions of NAR and NARX neural network for long-term wind speed forecasting in Malaysia," *Mathematical Problems in Engineering*, vol. 2019, Article ID 6403081, 14 pages, 2019.

[33] M. Dorofki, A. H. Elshafie, O. Jaafar, O. A. Karim, and S. Mastura, "Comparison of artificial neural network transfer functions abilities to simulate extreme runoff data," in *International Proceedings of Chemical, Biological and Environmental Engineering*, vol. 33, pp. 39–44, IACSIT Press, Singapore, International Conference on Environment, Energy and Biotechnology, 2012.

[34] R. Prasad, A. Pandey, K. P. Singh, V. P. Singh, R. K. Mishra, and D. Singh, "Retrieval of spinach crop parameters by microwave remote sensing with back propagation artificial neural networks: a comparison of different transfer functions," *Advances in Space Research*, vol. 50, no. 3, pp. 363–370, 2012.

[35] K. S. Prasad, S. R. Chalamalasetti, and N. R. Damera, "Application of grey relational analysis for optimizing weld bead geometry parameters of pulsed current micro plasma arc welded inconel 625 sheets," *The International Journal of Advanced Manufacturing Technology*, vol. 78, pp. 625–632, 2015.

[36] M. Srivastava, S. Maheshwari, T. K. Kundra, and S. Rathee, "Estimation of the effect of process parameters on build time and model material volume for FDM process optimization by response surface methodology and grey relational analysis," in *Advances in 3D Printing & Additive Manufacturing Technologies*, D. Wimpenny, P. Pandey, and L. Kumar, Eds., pp. 29–38, Springer, Singapore, 2017.

[37] B. Rajeswari and K. S. Amirthagadeswaran, "Experimental investigation of machinability characteristics and multi-response optimization of end milling in aluminium composites using RSM based grey relational analysis," *Measurement*, vol. 105, pp. 78–86, 2017.

[38] C. Naga Satya Kirti and M. V. Jagannadha Raju, "Optimization of process parameters in WEDM on inconel 600 using central composite design and grey relational analysis," in *Recent Advances in Material Sciences*, S. Pujari, S. Srikiran, and S. Subramonian, Eds., Lecture Notes on Multidisciplinary Industrial Engineering, pp. 397–407, Springer, Singapore, 2019.

[39] J. Deng, "Introduction to grey system," *The Journal of Grey System*, vol. 1, pp. 1–24, 1989.